International Journal of Radiology

Online Submissions: http://www.ghrnet.org/index./ijr/
doi:10.17554/j.issn.2313-3406.2015.02.5

Int Journal of Radiology 2015 June 2(1): 29-37
ISSN 2313-3406(print)

ORIGINAL ARTICLE

A Survey Over Image Quality Analysis Techniques for Brain MR Images

Luminița Moraru, Simona Moldovanu, Cristian Dragos Obreja

Luminița Moraru, Simona Moldovanu, Cristian Dragos Obreja, Faculty of Sciences and Environment, Department of Chemistry, Physics and Environment, Dunarea de Jos University of Galati, 47 Domneasca St., Galati, 800008, Romania

Simona Moldovanu, Dumitru Motoc High School, 15 Milcov St., 800509, Galati, Romania

Correspondence to: Luminița Moraru, Faculty of Sciences and Environment, Department of Chemistry, Physics and Environment, Dunarea de Jos University of Galati, 47 Domneasca St., Galati, 800008, Romania

Email: luminita.moraru@ugal.ro

Telephone: +40-336-130251

Received: February 10, 2015 Revised: April 22, 2015

Accepted: April 28, 2015

Published online: June 2, 2015

ABSTRACT

AIM: We carry out a study on image quality methods, organize them in a logical approach, provide the mathematical framework, and finally discuss their performance. Objective image quality measures are frequently used in image processing. This review is not dedicated to subjective tests as they are very difficult and time consuming processes.

MATERIALS AND METHODS: The quality studies are performed during the pre-processing step through the assessment of the de-noising efficacy, during the processing step as segmentation operation and as methods that evaluated its performance or in pattern-recognition. Extensive studies have taken hybrid metrics into account such as structural similarity index (SSIM), mean SSIM, feature similarity, the quality index based on local variance, and objective metrics such as signal-to-noise ratio, peak signal-to-noise ratio, mean square error, mean absolute error, contrast to noise ratio, root mean square error, Bhattacharyya coefficient or mutual information.

RESULTS: These methods are compared in the context of brain MR images based on the reported performances. The most frequently used objective metric in the evaluation of the quality of processed MR image is SNR because it is slightly tissue-depended. From the hybrid metrics, the most used is SSIM.

CONCLUSION: This paper summarized the objective and hybrids metrics that are Human Vision System - based characteristics. Also, it discusses on the notion of image quality assessment. The problems faced by various metrics are highlighted and the advantage of utilized a certain metric or a tandem of certain metrics are emphasized.

Key words: Image quality assessment; Hybrid metrics; Objective metrics; Signal-to-noise ratio; Contrast to noise ratio; Structural similarity index

Moraru L, Moldovanu S, Obreja CD. A Survey Over Image Quality Analysis Techniques for Brain MR Images. *International Journal of Radiology* 2015; 2(1): 29-37 Available from: URL: http://www.ghrnet.org/index.php/ijr/article/view/1068

INTRODUCTION

Magnetic Resonance Imaging (MRI) gives sound and detailed information about internal tissue structures and has a major influence in brain image analysis and diagnosis field. Three types of MR brain images, T1-weighted (T1w), T2-weighted (T2w) and proton-density weighted (PDw) that handles with different contrast characteristics of the brain tissues exist.

In the MR image acquisition terms, the data consist of both discrete Fourier samples, usually referred to as k-space samples and magnitude MR imaging, when the image phase is disregarded and only the magnitude is of interest. The magnitude images encompass the real and imaginary components of the "clean" data as well as the real and imaginary components of the noise with a certain variance. The noisy pixels in the magnitude image obey the Rician distribution and this Rician noise is signal-dependent[1]. The de-noising algorithms designed for additive white Gaussian noise reduction do not give good results on Rician image data[2].

Typically, MR images suffer from various artefacts as image inhomogeneity, noise (usually, Rician type), patient motion or extra cranial tissues that reduce the overall accuracy. All of these can lead to misinterpretation of brain MR data or even can hinder the practicians' access to the useful information. Brain disorder diagnosis and brain disorders classification by using MR images are specific medical image analysis methodologies that require a superior image quality. It is equally important to predict and to enhance the quality of the image. For these reasons, image quality assessment (IQA) is a challenging task for digital image processing. IQA can be done subjectively, objectively or in a hybrid approach (namely, based on the similarity with the Human Visual System (HVS) characteristics and coupled with objective measures) (Figure 1).

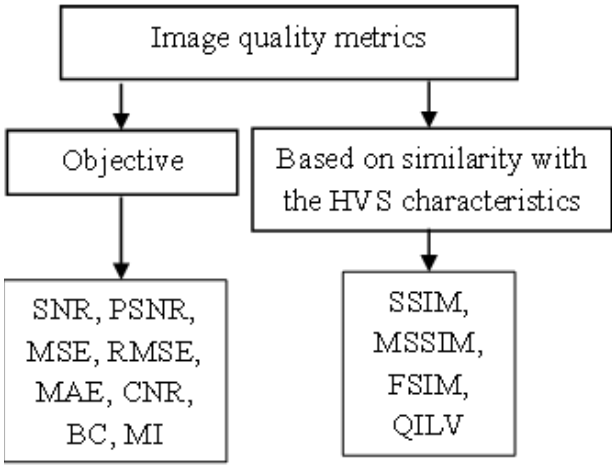

Figure 1 Image quality assessment.

The following abbreviations are used: SSIM- structural similarity index; MSSIM - mean SSIM; FSIM - Feature Similarity; QILV - the quality index based on local variance; SNR - signal-to-noise ratio; PSNR - peak signal-to-noise ratio; MSE - mean square error; MAE - mean absolute error; CNR - contrast to noise ratio; RMSE - root mean square error; BC - Bhattacharyya coefficient; and MI - mutual information.

All these evaluation techniques have their pros and cons. Many reports claim that the subjective evaluation is the best solution for IQA, but its main drawbacks consist of less speed, it is very expensive for current application and should be completed with objective methods for a reliable diagnostic. On the other hand, the objective image quality metrics show many advantages. They are fast and reproducible but require expensive software. Also, the objective IQA requires for a reference (ideal) image that is assumed to be 'the perfect image' from the quality point of view. The hybrid methods are based on the similarity with the human visual system HVS characteristics. They encompass some HVS features like: the sensitivity to lower spatial frequency, the sensitive to luminance contrast rather than the absolute luminance value and contrast masking that leads to a decrease in detectability of an image component vs. another. However, even these methods should be complemented with objective methods for a sound quality assessment.

Clinical acceptance of objective image quality assessment depends on its ability to predict the quality of brain MR image in a very similar way as the visual inspection as subjective assessment does.

IQA can be used in all stages of the processing pipeline of the brain MR images, namely during pre-processing, feature analysis, segmentation and post-processing. It can be used as benchmark tool to provide information about the best algorithm or as an optimization tool in de-noising and image restoration.

In this paper, an extensive comparative analysis is performed to illustrate the merits and demerits of various objective and hybrid image quality assessment techniques.

OBJECTIVE METRICS

1 Signal-to-noise ratio (SNR)

The SNR is a typical metric used to compare imaging hardware, acquisition or de-noising methods. It is slightly tissue-depended. Generally, the application of SNR is to compare the static images, such as images from two different coils or pulse sequences. This metric is equal to the ratio of the average signal intensity over the standard deviation of the noise, given in decibel (dB)[3]:

$$SNR = 10 \log \frac{\sum_{i=0}^{N-1}\sum_{j=0}^{M-1} f^2(i,j)}{\sum_{i=0}^{N-1}\sum_{j=0}^{M-1} (g(i,j)-f(i,j))^2} (\text{dB}) \qquad (1)$$

where *f(i,j)* is the original image and *g(i,j)* is the image corrupted by noise with M×N size.

An experiment focused on the functional MRI demonstrates that the SNR increases with the magnetic field strength. Thus, an increase of 10% or 13% for SNR has been reported when the magnetic field increased from 1.5 T to 3.0 T[3,4]. The main motivation to acquire MR images at higher field strengths is the possibility to have higher SNR values. In the high-magnetic field imaging, the dependence of the signal on field strength is not dominant. Another parameter that influences the SNR value is the MR image type. Voss *et al*[3] demonstrated that the relaxation time T1 increases and T2 remains almost constant when the field strength increases. In an early study, Parrish *et al*[5] analyzed the SNR variation in order to find the minimum optimal value able to allow the detection of the smaller fluctuations in the fMRI signals. The BOLD technique (Blood Oxygenation Level Dependent) that exploits the relationship hemodynamic variations - neuronal activity was used in order to detect the signal changes induced by brain activations. The requirement of this method was the SNR should be high enough to detect fMRI signal changes greater than 1%. This technique fails to detect signal changes of 1% or smaller near the lesion but highlights the clinical importance of SNR in fMRI experiment.

The SNR can be improved without sacrificing the spatial resolution using a new signal-preserving technique for noise suppression based on spectral subtraction method (SSD) proposed in[6]. The SSD method has been used in MR images, commonly degraded by additive Gaussian noise that shows a constant power spectrum. The noise was added to both real and imaginary parts of the 2D FT (in Fourier-domain computation). The noise power spectrum has been computed using the variance of the intensity values into the areas belonging to the background part of the image. Then, it has been subtracted from the original power spectrum in the Fourier domain in order to obtain the de-noised power spectrum. The SSD method could be used for images with artefacts induced by physiological noise and motion. This study reported a SNR improvement up to 45% for phantoms MRI, but it is comparable to the results provided by the anisotropic diffusion filtering method for real MRI.

Another sensitive method able to measure the microscopic motion of water molecules within tissue is the Diffusion Weighted Imaging (DWI). Even if, the diffusion weighted images are characterized by a low SNR, they contain a lot of biased data. Manjón *et al*[7] used

the Principal Component Analysis (PCA) during the de-noising operation. They proposed a local PCA de-noising method over small local windows instead of the whole image taking the advantage of the sparse representation. The method has been evaluated on both synthetic and real clinical images. The main improvements that the authors claim are related to the ability of the filter to remove not only the noise in multi-directional DWI data by using a local PCA-based decomposition but also the bias induced by the Rician noise; the resulted parameters better reflect the characteristics of the tissue.

A wavelet multiscale de-noising algorithm based on the Radon transform for MR images has been proposed by Yang and Fei[8]. The Rician nature of noise in MR images was taken into account. The main challenge of the Rician noise consists of its asymmetric probability density function for low signal intensities. The proposed method addressed to the darker region into MR images such as skull, nasal sinuses and cerebrospinal fluid, because these regions have the lower SNR. The authors have applied a Radon transform combined with a wavelet transform to the original images and have found that the sum of several Rician distributed noises has a symmetric distribution so the noise distribution has been identified with a Gaussian distribution. The authors stated that it is an effective de-noising method that allows the preservation of the important image details and features.

Another application of wavelet transform has been proposed by Scharcanski *et al*[9]. The main goal was the de-noising of the MR images with edge preservation based on scale and space consistency. The method combines the wavelet coring and the scale consistency by using a shrinkage function and space consistency through the geometric constrains (contour continuity and orientation continuity along consecutive levels). This method has been applied on the noisy images (SNR=8 dB and 3 dB). In the case of 3 dB noise, the de-noising operation with the proposed method achieves a SNR of 15 dB. The edges were preserved but some subtle details were lost. However, both visual and objective comparisons favor the proposed method. Various authors, e.g.[10-12] have also used wavelet analysis in de-noising operation to increase the image quality. In[12] a new approach for de-noising MR images with Rician noise using low complexity joint detection and estimation has been proposed. The authors introduce an analytical model for the probability of signal presence adapted to the global histogram coefficients and to a local indicator of spatial activity (assumed to be a locally averaged magnitude of the wavelet coefficients). A 3 × 3 window size was found to provide the best SNR values, for various K tunable parameters that control the notion of the signal of interest. It has been shown that the increase of K leads to a stronger suppression of the background texture and to an enhancement of sharp intensity variations.

Generally, a tradeoff between noise reduction and the preservation of key image features should exist with the final goal to enhance the diagnostically relevant image content.

2. Peak signal-to-noise ratio (PSNR)

The PSNR is a quality measure between the original and a distorted image. The peak signal to noise ratio, is computed as:

$$PSNR = 10\log \frac{N \cdot M \left(\max\limits_{i,j} f(i,j) \right)^2}{\sum\limits_{i=0}^{N-1} \sum\limits_{j=0}^{M-1} \left(g(i,j) - f(i,j) \right)^2} (\text{dB}) \qquad (2)$$

where *f(i,j)* is the original image and *g(i,j)* is the image corrupted by noise. The images have M×N size[13]. Generally, a higher PSNR denotes a better de-noising method and indicates a higher quality image. Some tests show that this statement is not always true. PSNR is useful only to compare the restoration results for the same image. In the case of between-image comparisons, PSNR is meaningless. In[14], the authors shown that the PSNR has to be used only for comparative quality assessment with fixed content.

In the scientific literature, PSNR focuses on the evaluation of the various de-noising methods that use various filters[13,15,16], wavelets[17,18] or are hybrid methods that corroborate filters with wavelets[19-21].

Two main strategies were developed for de-noising the magnitude of MR images. In the first approach, the Rician data are directly treated in the image domain. In the second, in order to avoid the difficulties raised from Rician noise, the de-noising operation works in the squared magnitude space. Here the signal spectrum is spreading and the bias associated with the Rician noise is better removed.

Mohan *et al*[13] proposed a new filter based on nonlocal neutrosophic set approach of Wiener filtering. Nonlocal means filter effectively reduces the noise while minimally affects the original structures of the image. A ω-Wiener filtering is employed and the entropy measures the indetermination degree of the image. A neutrosophic set image is characterized by a pixel that is transformed into the neutrosophic set domain namely, there are three probabilities: this pixel belongs to white pixels set, indeterminate set and non white pixels set, respectively. The reported performance of the de-noising nonlocal neutrosophic set vs. different de-noising methods (the PSNR values are put between brackets) is as follows: anisotropic diffusion filter (25.3 dB), Wiener filter (24.4 dB), total variation minimization scheme (24.5 dB) and nonlocal neutrosophic set (31.35 dB).

Tasdizen[15] reported an in-depth analysis of a variation of the non-local means (NLM) image de-noising method based on principal component analysis. Here, a set of eight images were used, including the brain MR images. The images were corrupted with additive Gaussian noise with standard deviation of 10, 25 and 50. Then, the images were improved using the proposed principal neighborhood dictionary (PND) method in the following image neighborhoods: 1×1, 3×3, 5×5, 7×7, 9×9 with respect to the PCA subspace dimensionality.

The use of an optimized NLM de-noising algorithm in conjunction with the squared-magnitude image was proposed by Hong *et al*[16]. This approach exploits so-called "Chi-square Unbiased Risk Estimate" which is a robust unbiased estimate of the expected mean-square error between the (unknown) noise-free squared-magnitude image and a processed version of it. Transverse, coronal and sagittal brain MR images are used to perform the optimization of proposed algorithm. The better PSNR values fall in the range from 24.01 dB to 35.63 dB. Each image was corrupted with various levels of Rician noise (5, 10, 20, 30 and 50).

In the wavelets application domain, many papers that focused on noise removal in clinical images or other physiological signals were published. Even if the wavelet transform are extensively used in filtering operations, they show some drawbacks such as oscillations, shift variance or aliasing. Raj and Venkateswarlu[17] proposed a de-noising approach of MR images using the dual tree complex wavelet transform for feature extraction and object recognition. A global threshold approach was used to remove the small absolute value coefficients that encode the noisy pixels and very fine details of the signal. The noise level has been established using the median absolute deviation and the de-noising efficiency has been evaluated based on PSNR. Although there are higher values of PSNR the quality of the images is not always very good. The artefacts as edge blur or ringing effect are removed by using discrete wavelet transform. Satheesh and Prasad[18] proposed a de-noising method based on contourlet transform (that can capture image edges and contours in an accurate way) in order to remove the Gaussian noise. PSNR metric has been used to

compare the performance of the method vs. the soft threshold and Wiener filter in the wavelet domain. According to their results, when the noise variance increases from 20 to 60, the PSNR decreases from 25 dB to 13 dB, and the proposed method outperforms the Wiener and wavelet filters.

Wiest-Daessle *et al*[19] proposed an improved version of the NLM filter to de-noise MR images affected by Rician noise. The quality of image restoration was evaluated by PSNR. They found that the PSNR values decrease when the Rician noise level increases. Also, the paper[20] focused on the improvement of the image quality by de-noising and resolution enhancement. The average, median and Wiener filters for image de-noising and discrete wavelet transform (DWT) and dual tree complex wavelet transform (DT-CWT) techniques for resolution enhancement have been used. The performance of de-noising was analyzed by PSNR and the following results were obtained: average (50.5dB), median (60.36 dB), DWT (57.34 dB), DT-CWT (61.9 dB) and Wiener filters (88.01 dB) [20]. Sukhatme and Verma[21] used the undecimated discrete wavelet transform (UDWT) to de-noise the MR images. Their results indicate that UDWT method improves the PSNR values from 21.43 dB to 26.70 dB (for a noise variance of 0.01) and MSSIM values from 0.9997 to 0.9998.

3. Mean square error (MSE)

The MSE is an error metrics that represents the cumulative squared error between the distorted and the original image. It is defined as:

$$MSE = \frac{1}{N \cdot M} \sum_{i=0}^{N-1} \sum_{j=0}^{M-1} \left(g(i,j) - f(i,j) \right)^2 \qquad (3)$$

where *f(x,y)* is the original image, *g(i,j)* is the degraded image with M×N size[13].

A lower MSE indicates lesser errors. Despite the fact that the MSE is very popular, it shows some drawbacks. Thus, it strongly depends on the image intensity scaling and the squared difference diminishes the small differences between the two pixels but penalizes the large ones. Also, it exhibits weak performance when assessing the perceptually signals such as speech and vision. Two distorted images can have the same MSE but may encompass different types of errors so, they may differ visibly.

In the literature, there are many papers that report various algorithms that have most often been compared using the MSE. Dua and Raj[22] proposed a wave atom shrinkage method as a de-noising tool of brain MR images degraded by Rician noise. Wave atom is a variant of 2D wavelet packets having better directional and decomposition capabilities. Using a new variant for threshold computation, this method assesses the efficacy of de-noising using a set of four parameters. In terms of MSE values, lower values are reported for the proposed method. Looking at another area of application, van der Kouwe *et al*[23] developed a method for 'on-line automatic slice positioning for brain MR imaging', in T1w environment, that used MSE as an evaluation tool of the automatic slice positioning. The performance of positioning in terms of individual translations and rotations has been analyzed using the maximum or minimum value of MSE between automatic alignment localizers and atlas of aligned brain images (as a standard).

Even if the MSE doesn't have good results during the quality assessment of the individual, it can be useful in the evaluation of the some anatomical structures that are present in all individuals, in an average manner. Hellier *et al*[24] used MSE as a global measure for evaluating average brain's volumes (in voxels) resulted from segmentation operations or for the overlap of the grey and white matter tissues as a measure of the deformation of the tissues during the image registration. It must be noted that the MSE is always complemented by other metric such as mutual information or correlation.

4. Root mean square error (RMSE)

Root mean square error is MSE-based on defined and it assesses the pixel difference between the original and the processed image:

$$RMSE = \sqrt{MSE} \qquad (4)$$

It amplifies and severely punishes large errors. Its values should be low for an efficient filtering operation as it examines the quantity of the removed noise. RMSE is a distance measure commonly used to measure the different filter performances[7]. Manjón *et al*[7] provided a de-noising analysis based on the following filters: nonlocal means, oracle-based 3D discrete cosine transform, wavelet sub-band mixing, rotationally invariant nonlocal means and compared their results with related state-of-the-art methods using RMSE and SSIM measures. The noise level varied from 0 to 15. Rizvi *et al*[25], performed a de-noising and segmentation study based on morphological filters and watershed method, respectively. The de-noising efficacy was analyzed using MSE and RMSE. The authors in[20,26] used their proposed methods and exploited the quality of image processing using RMSE metric, in the Rician noise assumption in brain MR images.

5. Mean absolute error (MAE)

In order to measure the distortions in an image and to compare the performance of certain processing operation, the mean absolute error that reflects the image fidelity could be considered[13]:

$$MAE = \frac{1}{N \cdot M} \sum_{i=0}^{N-1} \sum_{j=0}^{M-1} \left| g(i,j) - f(i,j) \right| \qquad (5)$$

Usually, MAE provides better results than the MSE and estimates either the image fidelity closer to a human viewer or the closeness of the images to each other. It belongs to pixel difference-based measures.

The MAE is a hallmark that can appraise the performance of various de-noising methods based on filters[27], wavelets[17,22] and kernel via PCA[15,28]. In the post-processing phase, MAE is used to evaluate the accuracy of segmentation and as an improvement tool of quantitative precision of segmentation[29]. Another application deals with the early identification of brain atrophy or anatomy deviating from the normal pattern based on automatically estimation of the age of healthy subjects from their T1w MRI scans[28]. The accuracy of the age estimations has been estimated using MAE and the authors found MAE to be the most meaningful measure for assessing the influence of different parameters (such as affine registration, the size of smoothing kernel and the values of spatial resolution).

6. Contrast to noise ratio (CNR)

CNR supports many different definitions depending how the signal of interest is identified. One way to define CNR deals with the difference between the mean values of the signals in two images or with the signal amplitude relative to the existing noise in an image. Also, CNR provides a measure of how much the SNR differs between different tissue types. It can be defined as[30]:

$$CNR = \frac{\mu(g(i,j)) - \mu(f(i,j))}{\sqrt{\frac{\sigma(g(i,j))^2 + \sigma(f(i,j))^2}{2}}} \qquad (6)$$

where μ and σ w are the mean and standard deviation, respectively, of the analyzed images of regions of interest. Its main goal is to obtain

an image having the higher CNR between pathological and normal tissues than in any of the initial images. The most used hypothesis when the CNR is analyzed, is those that the original and target images have the same noise weights. However, CNR depends on the pixels' location in the image so it could be not exactly identical among different calculations. The shortcomings of the contrast assessment come from the fact that if the contrast of an image is highly concentrated on a specific range, the information contained in the adjacent areas may be lost. Also, the edges presence into images could induce artifacts. CNR is most applicable when the mean grey scale of the signal is representative for the entire image. Usually, SNR and CNR are both used in evaluating the acquisition process of MRI; they are strongly influenced by the magnetic field strength.

In this context, the brain MR images that are strongly inhomogeneous will affect the CNR accuracy and the solution is to compute CNR in regions of interest. Usually, the following regions of interest are subject to analysis: grey matter, white matter, cerebrospinal fluid, air or background or various cerebral lesions[31-33]. Also, the contrast of brain MR images is strongly influenced by the T1 and T2 relaxation times of the specific tissues and by the magnetic field strength, temperature, scan parameters or the local and surrounding blood vessel distribution[3,34]. Magnotta *et al*[35] demonstrated that SNR and CNR increase at higher field strengths and they have large variation that represents a potential source of biased data.

7. Bhattacharyya coefficient (BC)

BC coefficient measures the similarity between the original image (target image) and modified image (query image). The Bhattacharyya distance is calculated between the histogram of the original image and the histogram of modified image. BC has associated a value of 1 between two images that have the same normalized histograms and 0 when they are completely dissimilar[30].

$$BC = \sum_{i=1}^{N} \sqrt{l(i) \cdot r(i)} \qquad (7)$$

where N denote the number of bins in the histogram (with the corresponding probabilities), l are the N-bins blocks of the original image and r are the N-bins blocks of the modified image. We can state that Bhattacharya coefficient belongs to the spectral methods. The main applicability of BC is in the field of color histograms to correlate images and this method produces biased results when it is applied to gray scale images. However, in the last years, BC has found application in measuring the dissimilarity of textures.

A wide number of works have included BC metric for medical image processing, analyze and quality evaluation. In the next paragraph some works based on the BC approach are shortly presented.

Udayakumar and Khanaa[36] proposed a method for an automatic diagnosis of dementia in T1w MR images based on Histogram Oriented Gradient as a feature extraction technique. Bhattacharyya distance and the Summed Euclidean distance were used for similarity measure between the query and target images.

Many semi-automatic, automatic or full automatic methods were implemented for detection of edemas and/or brain tumors. Generally, the BC has been coupled with PSNR, MSE or Pearson's correlation coefficient in order to detect various abnormalities caused by tumors and to localize them in the left or right hemispheres[37-39]. A semi-automatic method to segment the MS lesions was performed in[40]. The authors used a multiscale classification using a variational Dirichlet process and an active contours model based on statistical knowledge. In order to discriminate MS lesion, the BC has been used. In another work[41], BC measures similarity between two normalized gray level intensity histograms in order to automatically mark a tumor position and separate it from a healthy texture in brain MR images.

The detection of significant morphological differences of brain anatomy induced by brain atrophy in Alzheimer's disease has been performed by using the deformation-based morphometry method[42]. Some scalar measures of local deformations were followed by a supervised feature selection process that allows the feature data extraction for classification purpose. Feature selection was performed using the Pearson's correlation for voxel significance, Bhattacharyya distance that describes the class separability ability and the Welch's t-test statistic between two populations having unequal variances.

8. Mutual information (MI)

Mutual Information (MI) or relative entropy measures the degree of dependence of two discrete variables f and g that have the joint probability distribution of $p_{fg}(a,b)$ and the marginal distributions of $p_f(a)$ and $p_g(b)$. If the probability distributions are statistically independent, then $p_{fg}(a,b)=p_f(a)\bullet p_g(b)$. The degree of dependence is estimated by using the Kullback-Leibler measure[43]:

$$I(f,g) = \sum_{a,b} p_{fg}(a,b) \log \frac{p_{fg}(a,b)}{p_f(a) \cdot p_g(b)} \qquad (8)$$

Another interpretation of MI says that it is a measure of the amount of information one random variable contains about another. Namely, the regions of similar tissue (and similar gray tones) in one image would correspond to regions in the other image that also consist of similar gray values (but not the same as in the first image).

The primary application of the MI in medical image processing consists of the alignment or registration of multimodality images. Maes *et al*[43] used the MI to measure the statistical dependence or information redundancy between the image intensities of corresponding voxels in both images, with the final goal to completely automatic registration of multimodality medical images. They state that the MI of the image intensity values is maximal when the images are geometrically aligned. The same issue of registration is the subject of the paper[44]. The affine registration of brain images using inter-modal voxel similarity measures such as Correlation Ratio and Mutual Information is viewed as a global optimization method. Another practical application is to analyze serial structural MRI of the brain in the study of the neurodegenerative conditions when the localized changes in tissue intensity between time points exist[45]. The intensity or contrast effects, in serial MRI studies, may affect the accuracy of the registration. Studholme *et al*[45] focused on the regionally localizing mutual information and derived a single global criterion which is adapted to local tissue contrast. Their method allows an automated, sensitive and quantitative mapping of local tissue volume changes in the study of neuro-degeneration and development. The same maximization of mutual information approach was used in[46] for multimodal image registration. It modeled an image as a viscous fluid that deforms under the influence of forces derived from the gradient of the mutual information registration criterion. The method was validated on simulated T1w/T1w, T1w/T2w and T1w/PDw brain MR images with similar dimensions and voxel sizes. Better results were obtained when the T1w images were used as template images because the forces driving the registration depend on the gradient of the template image and T1w shows the higher gradient at the interface between GM and WM. The joint histogram of the two MR images was used to develop an approach dedicated to develop an artifact-free or nearly artifact-free MI-based registration algorithm to improve registration accuracy[47]. The joint histogram of an image pair was

defined as a function of two variables, the gray-level intensity in the first image and, the gray-level intensity in the second image. The joint histogram counts how many times each gray-level correspondence occurs. If the images are correctly registered, the joint histogram shows certain clusters for gray-levels of matching structures.

METHODS HYBRID METRICS BASED ON HVS CHARACTERISTICS

1. Structural similarity index (SSIM)

The structural similarity index (SSIM) measures the structural similarity of a processed image against a reference image or the preservation degree of the relevant structures. SSIM has found many applications from image classification[48-51], restoration and fusion[52], to watermarking, de-noising and biometrics[53].

Δ1, Δ2) in the set of coordinates, Δ2, its local neighbourhood of radius r is defined as Δ2, Δ-Δ1⩽Δ}. For two spatial locations *x* and y, the SSIM is defined as:

Δ, Δ=2ΔΔ+Δ1Δ2+Δ2+Δ1+2ΔΔΔΔ+Δ2ΔΔ2+ΔΔ2+Δ2ΔΔΔ,Δ+3ΔΔΔ Δ+Δ3Δ=Δ(Δ,Δ)ΔΔ(Δ,Δ)ΔΔ)(Δ,Δ)Δ (9)

Δ and Δ denote the mean valuse, ΔΔ and ΔΔ are the standard deviation and ΔΔΔ is the Δ1, Δ2 and Δ3 are small positive constants. The luminance and contrast terms describe the non-structural distortions, and the last term (structural distortion) characterizes the loss of linear correlation. SSIM satisfies the following conditions:

1. symmetry: *SSIM* (*x*; *y*) = SSIM (*y*; *x*)
2. boundedness: SSIM (*x*; *y*) ⩽1
3. unique maximum: SSIM (*x*; *y*) =1 if and only if $x = y$.

Chincarini *et al*[54] used in their paper a local application of this metric when noise filtering procedure has been develop for 3D images. They looked for the appropriate three thresholds of the principal slices (axial, sagittal, coronal) passing through the image center of mass. The local image patches taken from the same location of two images g and f provide three elements used to compute the structural similarity index: the local patch luminance, the local patch contrast, and the local patch structure. The final metric is given by the average of the local metrics computed for the principal slices

Manjón *et al*[7] proposed two methods for de-noising 3D MR images that used the sparseness and self-similarity properties of the images. They adopted the discrete cosine transform DCT that uses the sparseness of the image (i.e., the ability of the image to be represented by a small number of base functions) and a NLM filter approach that uses the pattern redundancy. In the case of DCT filtering method, the parameter was a is the standard deviation of the Rician noise). For the second approach, parameter. The SSIM has been estimated using the following constants, $c_1=(k_1L)^2$ and $c_2=(k_2L)^2$ (where *L* is the dynamic range, k_1=0.01 and k_2=0.03) and a Gaussian kernel of 3×3×3 voxels. The results were evaluated in a comparative way for different image types and noise levels, using SSIM and RMSE in T1w and PDw.

Various methods for noise filtering in MR images that follow a Rician model were adopted. In[55], a variant of the linear minimum mean square error estimator for noise with Rician distribution has been proposed. Both the parameters of Rician distribution (using a single magnitude image and multiple images) and the signal were estimated. By using the SSIM, the authors proved that the proposed de-noising method allowed for good edge and structural information preservation. The quality measures for synthetic experiment were compared with the results provided by maximum likelihood approach, expectation maximization formulations, Koay method[56] and Wiener and wavelet based filters. In[57], the Poisson and Rician noise distribution were transformed into Gaussian distribution using variance stabilization method. After that, a patch-based algorithm allows for de-noising the images. SSIM performs the image quality assessment using the same parameters by default. Aja-Fernandez *et al*[58] performed an assessment of the image quality by comparing the local variance distribution of two images. Some distortions as blur and noise are inserted into images and then, the image quality has been estimated using the local variance distribution because it encompasses a great amount of the structural information. The authors showed that the weakness of SSIM consist of that it calculates the local variances of both images, but the index provides information only on the mean of those values. A new variant of this index has been proposed, namely the Quality Index based on Local Variance (QILV), and it encompasses the local statistics of the images based on the local variance of an image. The authors claimed that the performances of this new index correspond more closely to those expected from subjective visual assessment (concerning structural information). However, there exists a drawback of their method. The size of the neighborhood used to weight the local variance should be defined according to the particular application.

2. Mean structural similarity index metrics (MSSIM)

Various approaches have been explored in developing algorithms for structural similarity measurements. Mean structural similarity index metrics is an extension of SSIM. If a $k \times k$ window moves across an image, a local SSIM score is calculated. If the entire image is taken into account, a simple arithmetic average of each of the local scores is referred as the mean SSIM[59].

$$MSSIM = \frac{1}{M}\sum_{j=1}^{M} SSIM\left(f_j, g_j\right) \qquad (10)$$

Wang *et al*[59] demonstrated that images having the same MSE may show strong different image quality. It seems that MSE is highly sensitive to changes in luminance and contrast while SSIM is highly sensitive to noise. The proposed MSSIM adapt better to perceptual evaluation, namely for images that have almost the same MSE but have different quality. However, both SSIM and MSSIM may fail in the evaluation of noisy, blurred or compressed images when the completely different images are indicated as similar. MSSIM is an attempt to balance the characteristic of the structural index that measures the variations in luminance and contrast separately, so that the overall MSSIM index should be not affected by such changes.

Based on this property, various de-noising methods were proposed and MSSIM index has been used to compare the performance[21,26,60-62]. Also, the quality of compressed images used during the transmission stage or for storage purposes was investigated based on the MSSIM index[63]. Pursuing a multi resolution decompositions approach, Beladgham *et al*[63] investigated the MRI image compression based on a Cohen-Daubechies-Feauveau symmetric biorthogonal wavelet transform CDF 9/7 coupled with set partitioning in hierarchical trees (SPIHT) coding algorithm that allow to increase the image quality. The wavelet has a low pass associated filter that is characterized by 9 analysis coefficients and 7 synthesis coefficients. They have compared the results of compression obtained with wavelet based filters bank through PSNR and MSSIM indexes. The bit-rate or number of bits per pixel varied from 0.125 to 2 and, accordingly, the PSNR increases from 24.50 dB to 43.88 dB and MSSIM increases from 0.68 to 0.98. The performance of the method has been compared with different types of wavelet transforms such as wavelet Le Gall (lifting scheme) transform, CDF9/7 (lifting scheme) coupled with the SPIHT coding or CDF9/7 (Lifting scheme) combined with the embedded zerotree wavelet algorithm.

3. Quality index based on local variance (QILV)

In the brain MRI analysis, the spatial context incorporates the useful information for brain MRI understanding tasks. Each intensity pixel is highly statistically dependent on the intensities of its neighbors.

The universal QILV is a variant of statistical similarity metric. It is a complementary method based on the computation of the local variance distribution between two images. The modification made to the similarity index to improve the performance was based on the idea that a great amount of the structural information is hidden in the distribution of its local variance[13,64]. The QILV between two images f and g has been defined as:

$$QILV(f,g)=\frac{2\mu_f\mu_g}{\mu_f^2+\mu_g^2}\cdot\frac{2\sigma_f\sigma_g}{\sigma_f^2+\sigma_g^2}\cdot\frac{\sigma_{fg}}{\sigma_f\sigma_g} \qquad (11)$$

where μ_f, μ_g, σ_f, σ_g and σ_{fg} are the similar values like those of SSIM index[64]. The first term compares the mean of the local variance distributions of both images. The second one compares the standard deviation of the local variances and the last term introduces the spatial coherence. Generally, QILV accounts for structures/edges preservation.

The local variance of an image *f* is defined to be the sample variance of the collection of pixels centered at the considered pixel. It is defined into local neighborhood and it is weighted. The size of the neighborhood should be related to the scale of the image structures. This can be seen as constrain. However, Aja-Fernandez *et al*[58] pointed out that the proposed QILV index enhances the structural content at the expense of removing background information. This is a drawback in the case of MR images, because distinctive local contexts are important and should be preserved from the visual quality point of view.

The QILV is classified as a non-ROI-based measure by Sinha and Ramakrishnan[65] because the entire image is analyzed when the quality is determined. Tristán-Vega *et al*[66] used the popular NLM filter to reduce the noise in the MR images. Their method is an improved approach based on the difference between salient features associated to the pixels to be weighted. Prior to de-noising with NLM, the distance between patches was efficiently estimated by using a small subset of features and providing a fixed value to the parameter h (that is related to the noise power of the image). Also, they weighted average of all similar patches for a candidate patch. QILV has been used to estimate the performance of the proposed method. This quality index estimates the blurring degree of the structural information but a set of quality indexes has been used. QILV was correlated to the RMSE and SSIM values in order to estimate the real quality of brain MR images as filter outputs.

4. Feature Similarity Index (FSIM)

Based on the fact that HVS is very sensitive to the low-level features of an image such as edges or zero-crossing, Zhang *et al*[67] proposed a new quality index called feature similarity index. FSIM is a full-referenced metric and it is defined as follows:

$$FSIM=\frac{\sum_{x\in\Omega}S_L(x)PC_m(x)}{\sum_{x\in\Omega}PC_m(x)} \qquad (12)$$

where Ω defines the entire image spatial domain. The similarity measure $SL(x)$ combines the similarity measures of phase congruency (PC) and of gradient magnitude (GM):

$$S_{PC}(x)=\frac{2PC_1(x)\cdot PC_2(x)+\varepsilon_1}{PC_1^2(x)+PC_1^2(x)+\varepsilon_1}\ \text{and}\ S_G(x)=\frac{2G_1(x)\cdot G_2(x)+\varepsilon_2}{G_1^2(x)+G_2^2(x)+\varepsilon_2} \qquad (13)$$

where ε_1 and ε_2 ensure the stability of defined functions. When two images are compared in terms of feature similarity, the maximum value of phase congruency PC_m is considered. For all the distortion types involved in their study, FSIM outperformed the other quality indexes as SSIM, MS-SSIM or PSNR.

Phophalia *et al*[26] explored the patch based de-noising method through the rough set theory. This method works with the notion of granules that defined sets of neighboring pixels. In this way, an image is divided in distinct and separate small granules that allow for gathering detailed information and to build various classes that will be used in further analysis. Their approach considers the adjacent boundary information between objects in order to determine similar patches. FSIM was one of the comparative metrics used to assess the efficacy of de-noising.

Based on the finding that FSIM failed to consider various visual masking effects, Wang *et al*[68] proposed an improvement of FSIM index by considered the CSF (contrast sensitivity function) operator and the contrast masking operator in discrete cosine transform (DCT) domain. They demonstrated that the improved quality metric achieved higher consistency with the human subjective perception and it is superior to other relevant state-of-the-art image quality assessment metrics.

DISCUSSIONS

Despite of the multiple advantages offered by MRI technique, it shows some pitfalls as the noise presence or the non-standardized intensity, namely the MRI pixel intensities have no fixed value on the targeted tissue. In related words, pixels depicting the same tissue have different intensities in different slices, and false basis are created for computational analyses that used pixels intensity values. To overcome these drawbacks, various images processing tools and methods had been proposed in the past. Also, quantitatively assessment of the quality of the brain MR images was and remains a hot topic. Certain mathematical tools are essentially in the evaluation of the quality of the processed brain MRI. These metrics are classified as objectives, hybrid or subjective quality descriptors.

According to the information provided in Table 1, the most frequently used objective metric in the evaluation of the quality of processed MR image is SNR. The reason is that SNR is slightly tissue-depended. From the hybrid metrics, the most used is SSIM. If the value of SSIM is close to 1 the analyzed images tent to be similar.

Table 1 The searched items according to keywords from PubMed Database.

Metric	Searched terms	Number of items
SNR	Signal-to-noise ratio brain MRI	1681
PSNR	Peak signal-to-noise ratio brain MRI	65
MSE	Mean square error brain MRI	85
RMSE	Root mean square error brain MRI	48
MAE	Mean absolute error brain MRI	33
CNR	Contrast to noise ratio brain MRI	695
BC	Bhattacharyya coefficient brain MRI	3
MI	Mutual information brain MRI	246
SSIM	Structural similarity index brain MRI	15
MSSIM	Mean structural similarity index brain MRI	2
QILV	The quality index based on local variance brain MRI	1
FSIM	Feature similarity index brain MRI	5

CONCLUSION

The principal objective of this survey was to provide an overview of the available brain MRI metrics and on their applicability and limitations in the evaluation of the quality of the processed images. This paper summarized the objective and hybrids metrics that are HVS-based characteristics. Also, it discusses on the notion of IQA. The problems faced by various metrics are highlighted in the present study. Also, the advantage of utilized a certain metric or a tandem of certain metrics are emphasized.

ACKNOWLEDGEMENTS

The author Simona Moldovanu would like to thank the Project PERFORM, ID POSDRU/159/1.5/S/138963 of "Dunărea de Jos" University of Galați, Romania for support.

CONFLICT OF INTERESTS

There are no conflicts of interest with regard to the present study.

REFERENCES

1. Gudbjartsson H, Patz S. The Rician distribution of noisy MRI data. Magnet Reson Med 1995; 34: 910–914
2. Yang J, Fan J, Ai D, Zhou S, Tang S, Wang Y, Brain MR image denoising for Rician noise using pre-smooth non-local means filter. Biomed Eng Online 2015; 14(2): 14-22
.3. Voss HU, Zevin JD, Mc Candliss BD. Functional MR imaging at 3.0 T versus 1.5 T: A Practical Review. Neuroimag Clin N Am 2006; 16: 285–297
4. Jerrolds J, Keene S. MRI safety at 3T versus 1.5T. Internet J World Health Soc Politics 2009; 6: 1-8
5. Parrish TB, Gitelman DR, LaBar KS, Mesulam M. Impact of signal-to-noise on functional MRI. Magnet Reson Med 2000; 44:925–932
6. Priyadharsini B. A novel noise filtering technique for denoising MRI images. ICGICT 2014; 2(1): 2428-2433
7. Manjon JV, Coupe P, Concha L, Buades A, Collins DL, Robles M. Diffusion weighted image denoising using overcomplete local PCA. PLoS One 2013; 8: 1-12
8. Yang X, Fei B. A wavelet multiscale denoising algorithm for magnetic resonance images. Meas Sci Technol 2011; 22: 025803–025815
9. Scharcanski J, Jung CR, Clarke RT. Adaptive image denoising using scale and space consistency. IEEE Trans Image Process 2002; 11(9):1092 – 1101
10. Dinov ID, Mega MS, Thompson PM, Woods RP, Sumners DWL, Sowell EL, Toga AW. Quantitative comparison and analysis of brain image registration using frequency-adaptive wavelet Shrinkage. IEEE Trans Inf Technol Biomed 2002; 6(1): 73-85
11. Xue JH, Pizurica A, Philips W, Kerre E, Walle RVD, Lemahieu I. An integrated method of adaptive enhancement for unsupervised segmentation of MRI brain images. Pattern Recogn Lett 2003; 24: 2549-2560
12. Pizurica A, Philips W, Lemahieu I, Acheroy M. A versatile wavelet domain noise filtration technique for medical imaging. IEEE Trans Med Imaging 2003; 22(3): 323-331
13. Mohan J, Krishnaveni V, Yanhui G. MRI denoising using nonlocal neutrosophic set approach of Wiener filtering. Biomed Signal Process Control 2013; 8: 779– 791
14. Korhonen J, You J. Peak signal-to-noise ratio revisited: Is simple beautiful? QoMEX 2012; 137 – 38
15. Tasdizen T. Principal neighborhood dictionaries for nonlocal means image denoising Trans Img Proc 2009; 18(12): 2649-2660
16. Hong JO, Luisier F, Wolfe PJ. Magnitude MR image denoising via CURE-optimized non-local means. ISBI 2012; 141: 610-613
17. Naga V, Raj P, Venkateswarlu T. Denoising of medical images using dual tree complex wavelet transform. Procedia Technology 2012; 4: 238-244
18. Satheesh S, Prasad K, Medical Image Denoising using adaptive threshold based on contourlet transform. ACIJ 2011; 2(2): 52-58
19. Wiest-Daessle N, Prima S, Coupe P, Morrissey SP, Barillot C. Rician noise removal by non-local means filtering for low signal-to-noise ratio MRI: applications to DT-MRI. MICCAI 2008; 22: 171–179
20. Kumar MV, Madhu Kiran SP. Multi-Resolution analysis based MRI image quality analysis using DT-CWT based preprocessing techniques. Int J Eng Res Gen Sci 2014; 2(5): 768-775
21. Sukhatme N, Verma M. Denoising of magnetic resonance images using wavelet domain transform based methods. IJSRET 2012; 1(4): 031-038
22. Dua G, Raj V. MRI. Denoising using waveatom shrinkage global. J Electrical Electron Eng Res 2012; 12(4): 1-5
23. Van der Kouwe JW, Benner T, Fischl B, Schmitt F, Salat DH, Harder M, Sorensen AG, Dale AM. On-line automatic slice positioning for brain MR imaging. NeuroImage 2005; 27: 222-230
24. Hellier P, Barillot C, Corouge I, Gibaud B, Le Goualher G, Collins DL, Malandain AEG, Ayache N, Christensen GE, Johnson HJ. Retrospective evaluation of intersubject brain registration. IEEE Trans Med Imaging 2003; 22(9): 1120-1130
25. Rizvi ST, Sandhu MS, Fatima SF. Image segmentation using improved watershed algorithm. IJCSIT 2014; 5(2): 2543-2545
26. Phophalia A, Rajwade A, Mitra SK. Rough set based image denoising for brain MR images. Signal Proc 2014; 103: 24-35
27. Agrawal S, Sahu R. Wavelet based MRI image denoising using thresholding techniques IJSETR 2012; 1(3): 32-35
28. Franke K, Ziegler G, Klöppel S, Gaser C. Estimating the age of healthy subjects from T1-weighted MRI scans using kernel 2 methods: Exploring the influence of various parameters. NeuroImage 2010; 50(3): 883–892
29. Noe A, Gee JC. Partial volume segmentation of cerebral MRI scans with mixture model clustering Inf Process Med Imaging 2001; 2082: 423-430
30. Gonzalez RC, Woods RE, Digital image processing, 3th ed. London, Prentice Hall, 2008: 102-203
31. Weiskopf N, Mathiak K, Bock SW, Scharnowski F, Veit R, Grodd W, Goebel R, Birbaumer N. Principles of a brain-computer interface (BCI) based on real-time functional magnetic resonance imaging (fMRI). IEEE Trans Bio Med Eng 2004; 51(6): 230-237
32. Biswas J, Nelson CB, Runge VM, Wintersperger BJ, Baumann SS, Jackson CB, Patel T. Brain tumor enhancement in magnetic resonance imaging: comparison of signal-to-noise ratio (SNR) and contrast-to-noise ratio (CNR) at 1.5 versus 3 tesla. Invest Radiol 2005; 40(12): 792-797
33. Flacke S, Fischer S, Scott MJ, Fuhrhop RJ, Allen JS, McLean M, Winter P, Sicard GA, Gaffney PJ, Wickline SA, Lanza GM. Novel MRI contrast agent for molecular imaging of fibrin implications for detecting vulnerable plaques. Circulation 2001; 104(11):1280-1285
34. Uhrig L, Ciobanu L, Djemai B, Le Bihan D, Jarraya B. Sedation agents differentially modulate cortical and subcortical blood oxygenation: Evidence from ultra-high field MRI. PLoS One 2014; 9(7): 1-7
35. Magnotta VA, Friedman L. Measurement of signal-to-noise and contrast-to-noise in the fBIRN multicenter imaging study. J Digit Imaging 2006; 19(2): 140–147
36. Udayakumar R, Khanaa V. Dementia disease diagnosis in magnetic resonance imaging, MEJSR 2014; 20(9): 1055-1058
37. Dvorák P, Kropatsch WG, Bartušek K. Automatic brain tumor detection in T2-weighted magnetic resonance images. Meas Sci Rev 2013; 13(5): 223-230

38. Saha BN, Ray N, Greiner R, Murtha A, Zhang H. Quick detection of brain tumors and edemas: A bounding box method using symmetry. Comput Med Imag Grap 2012; 36: 95-107
39. Dluhos P, Schwarz D, Kasparek T. Wavelet Features for Recognition of First Episode of Schizophrenia from MRI Brain Images. Radioengineering 2014; 23(1): 274-281
40. Derraz F, Peyrodie L, Piniti A, Taleb-Ahmed A, Chikh A, Hautecoeur P. Semi-automatic segmentation of multiple sclerosis lesion based active contours model and variational Dirichlet process. CMES 2010; 67(2): 95-116
41. Fazli S, Nadirkhanlou P. A novel method for automatic segmentation of brain tumors in MRI images. IJASCSE 2013; 2(6): 1-6
42. Savio A, Graña M. Deformation based feature selection for computer aided diagnosis of Alzheimer's disease. Expert Syst Appl 2013; 40(5): 1619-1628
43. Maes F, Collignon A, Vandermeulen D, Marchal G, Suetens P. Multimodality image registration by maximization of mutual information. IEEE Trans Med Imag 1997; 16(2): 187-198
44. Jenkinson M, Smith S. A global optimisation method for robust affine registration of brain images. Med Image Anal 2001; 5: 143–156
45. Studholme C, Drapaca C, Iordanova B, Cardenas V. Deformation-based mapping of volume change from serial brain MRI in the presence of local tissue contrast change. IEEE Trans Med Imag 2006; 25(5): 626-639
46. D'Agostino E, Maes F, Vandermeulen D, Suetens P, A viscous fluid model for multimodal non-rigid image registration using mutual information. Med Image Anal 2003; 7: 565-575
47. Chen HM, Varshney PK. Mutual information-based CT-MR brain image registration using generalized partial volume joint histogram estimation. IEEE Trans Med Imag 2003; 22(9): 1111-1119
48. Gao Y, Rehman A, Wang Z. CW-SSIM Based image classification. ICIP 2011; 1249-1252
49. Channappayya SS, Bovik AC, Caramanis C, Heath R. Design of linear equalizers optimized for the structural similarity index. IEEE Trans Image Process 2008; 17(6): 857-872
50. Wang Z, Li Q, Shang X. Perceptual image coding based on a maximum of minimal structural similarity criterion. ICIP 2007; 2: 121-124
51. Rehman A, Wang Z. SSIM-based non-local means image denoising. ICIP 2011; 217-220
52. Piella G, Heijmans H. A new quality metric for image fusion. ICIP 2003; 3:173–176
53. Wang Z, Bovik AC. Mean squared error: love it or leave it? A new look at signal fidelity measures. IEEE Signal Process Mag 2009; 26: 98-117
54. Chincarini A, Bosco P, Calvini P, Gemme G, Esposito M, Olivieri C, Rei L, Squarcia S, Rodriguez G, Bellotti R, Cerello P, De Mitri I, Retico A, Nobili F. Local MRI analysis approach in the diagnosis of early and prodromal Alzheimer's disease. NeuroImage 2011; 58: 469–480
55. Aja-Fernández S, Alberola-López C, Westin CF. Noise and signal estimation in magnitude MRI and Rician distributed images: a LMMSE Approach. IEEE Trans Imge Process 2008; 17(8): 1383-1397
56. Koay CG, Basser PJ, Analytically exact correction scheme for signal extraction from noisy magnitude MR signals, J Magn Reson 2006; 179: 317–322
57. Prudhvi Raj VN, Venkateswarlu T. Denoising of magnetic resonance and x-ray images using variance stabilisation and patch based algortithms. IJMA 2012; 4(6): 53-71
58. Aja-Fernandez S, Estepar RSJ, Alberola-Lopez C, Westin CF. Image quality assessment based on local variance. EMBS 2006; 4815-4818
59. Wang Z, Bovik AC, Sheikh HR, Simoncelli EP. Image quality assessment: From error visibility to structural similarity. IEEE Trans Image Process 2004; 13(4): 600-612
60. Zhang M, Mou X, Zhang L. Non-shift edge based ratio: An image quality assessment metric based on early vision features. IEEE Signal Proc Let 2011; 18(5): 315-318
61. Yi Y, Yu X, Wang L, Yang Z. Image quality assessment based on structural distortion and image definition. CSSE 2008; 253-256
62. Komal A, Khurana S, Kumar A. Comparative analysis of image quality assessment using HVS model. IJIRCCE 2014; 2(7): 5033-5038
63. Beladgham M, Bessaid A, Lakhdar AM, Taleb-Ahmed A, Improving quality of medical image compression using biorthogonal CDF wavelet based on lifting scheme and SPIHT coding. Serb J Electr I Eng 2011; 8(2): 163-179
64. Muñoz-Moreno E, Aja-Fernández S, Martin-Fernandez M. Quality assessment of tensor images, tensors in image processing and computer vision. ACVPR 2009; 1:79-103
65. Sinha N, Ramakrishnan AG. Quality assessment in magnetic resonance images. Crit Rev Biomed Eng 2010; 38: 127-141
66. Tristán-Vega A, García-Pérez V, Aja-Fernández S, Westin CF. Efficient and robust nonlocal means denoising of MR data based on salient features matching. Comput Meth Prog Bio 2012; 105:131-144
67. Zhang L, Zhang L, Mou X, Zhang D. FSIM: a feature similarity index for image quality assessment. IEEE Trans Image Process 2011; 20(9): 2378–2386
68. Wang Z, Li Z, Lin W, Liu C. Image quality assessment based on improved feature similarity metric. APSIPA 2011; 1-5

Peer reviewer: Jürgen Hänggi, PhD, Division Neuropsychology, Department of Psychology, University of Zurich, Binzmuehlestrasse 14 / P.O. 25, CH-8050 Zurich, Switzerland.